VLM-R^3: Region Recognition, Reasoning, and Refinement for Enhanced Multimodal Chain-of-Thought

Chaoya Jiang[1*], **Yongrui Heng**[1*], **Wei Ye**[1†], **Han Yang**[3], **Haiyang Xu**[2†]
Ming Yan[2], **Ji Zhang**[2], **Fei Huang**[2], **Shikun Zhang**[1]
[1] National Engineering Research Center for Software Engineering, Peking University
[2] Alibaba Group
[3] ZEEKR Intelligent Technology Holding Limited
{wye}@pku.edu.cn,
{shuofeng.xhy}@alibaba-inc.com

Abstract

Recently, reasoning-based MLLMs have achieved a degree of success in generating long-form textual reasoning chains. However, they still struggle with complex tasks that necessitate dynamic and iterative focusing on and revisiting of visual regions to achieve precise grounding of textual reasoning in visual evidence. We introduce **VLM-R**^{3} (**V**isual **L**anguage **M**odel with **R**egion **R**ecognition and **R**easoning), a framework that equips an MLLM with the ability to (i) decide *when* additional visual evidence is needed, (ii) determine *where* to ground within the image, and (iii) seamlessly weave the relevant sub-image content back into an interleaved chain-of-thought. The core of our method is **Region-Conditioned Reinforcement Policy Optimization (R-GRPO)**, a training paradigm that rewards the model for selecting informative regions, formulating appropriate transformations (e.g. crop, zoom), and integrating the resulting visual context into subsequent reasoning steps. To bootstrap this policy, we compile a modest but carefully curated Visuo-Lingual Interleaved Rationale (VLIR) corpus that provides step-level supervision on region selection and textual justification. Extensive experiments on MathVista, ScienceQA, and other benchmarks show that VLM-R^3 sets a new state of the art in zero-shot and few-shot settings, with the largest gains appearing on questions demanding subtle spatial reasoning or fine-grained visual cue extraction.

1 Introduction

Multimodal Large Language Models (MLLMs) have recently emerged as a powerful paradigm, demonstrating remarkable capabilities in understanding and generating content across different modalities, primarily vision and language [37, 26, 22, 61, 5, 7]. Models like O1 [36], QvQ [3], and Gemini 2.5 [1] have showcased impressive performance on a wide array of tasks such as MMMU [62], MathVista [29], and ScienceQA [30]. A key factor contributing to their advanced reasoning abilities is the integration of Chain-of-Thought (CoT) prompting [55], which elicits step-by-step reasoning pathways, often leading to more accurate and interpretable outputs.

Despite these advancements, a critical limitation persists in the way current MLLMs interact with visual information during complex reasoning processes. Most existing approaches [3, 36, 57, 58]

[*] These authors contributed equally to this work.
[†] corresponding authors.

Preprint. Under review.

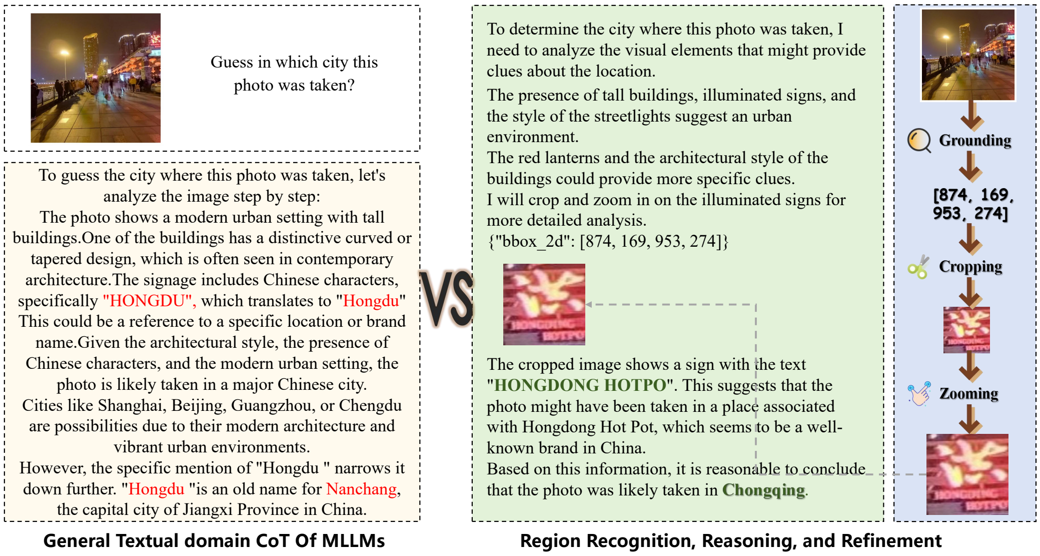

Guess in which city this photo was taken?

To guess the city where this photo was taken, let's analyze the image step by step:
The photo shows a modern urban setting with tall buildings.One of the buildings has a distinctive curved or tapered design, which is often seen in contemporary architecture.The signage includes Chinese characters, specifically "HONGDU", which translates to "Hongdu" This could be a reference to a specific location or brand name.Given the architectural style, the presence of Chinese characters, and the modern urban setting, the photo is likely taken in a major Chinese city.
Cities like Shanghai, Beijing, Guangzhou, or Chengdu are possibilities due to their modern architecture and vibrant urban environments.
However, the specific mention of "Hongdu " narrows it down further. "Hongdu "is an old name for Nanchang, the capital city of Jiangxi Province in China.

To determine the city where this photo was taken, I need to analyze the visual elements that might provide clues about the location.
The presence of tall buildings, illuminated signs, and the style of the streetlights suggest an urban environment.
The red lanterns and the architectural style of the buildings could provide more specific clues.
I will crop and zoom in on the illuminated signs for more detailed analysis.
{"bbox_2d": [874, 169, 953, 274]}

The cropped image shows a sign with the text "**HONGDONG HOTPO**". This suggests that the photo might have been taken in a place associated with Hongdong Hot Pot, which seems to be a well-known brand in China.
Based on this information, it is reasonable to conclude that the photo was likely taken in **Chongqing**.

VS
Grounding
[874, 169, 953, 274]
Cropping
Zooming
HONGDONG HOTPO
General Textual domain CoT Of MLLMs
Region Recognition, Reasoning, and Refinement

Figure 1: This figure visualizes the contrast between traditional text-based CoT reasoning and our proposed VLM-R^3 approach, which integrates region grounding and refinement in an interleaved visual-textual reasoning chain. While conventional text-based reasoning fails when analyzing scenes that require dynamic, iterative, and fine-grained interaction with specific visual regions, our approach succeeds by precisely identifying and focusing on critical visual elements, such as the ’Hongdong Hotpot’ sign in this example, to derive accurate conclusions through targeted visual reasoning.

employing CoT predominantly confine the reasoning steps to the textual domain, with only an initial static grounding in the visual input. This paradigm falls short in scenarios demanding dynamic, iterative, and fine-grained interaction with specific visual regions throughout the reasoning chain. As shown in Figure 1, examples include sequentially verifying hypotheses against image details, tracking object states across visual cues, or comprehending intricate spatial relationships—all of which require a more active and adaptive visual grounding mechanism. Encouragingly, recent models such as O3 [2] which capable of interleaving image analysis with text generation—inspire a new frontier where reasoning is not merely conditioned on an image, but is continuously intertwined with ongoing visual perception and localization.

Developing an MLLM that can “look again” during reasoning faces two notable hurdles: **Region-grounding learning.** The model must learn *where* to focus and *how* to transform the grounded region (crop, zoom) based on partial textual deliberation. **Credit assignment.** Simply supervising final answers does not teach the model whether a chosen region actually contributed to correct reasoning, making it hard to refine the visual-query policy.

To bridge this crucial gap, we make two primary contributions. First, we introduce Visuo-Lingual Interleaved Rationale (VLIR), a pioneering dataset meticulously curated to support the development of MLLMs for interleaved text-image CoT reasoning. VLIR provides explicit annotations for visual region localization, image cropping instructions, and semantic enhancement cues, all embedded within multi-step reasoning narratives. Second, building upon this, we propose **VLM-R**^{3} (**V**isual **L**anguage **M**odel with **R**egion **R**ecognition and **R**easoning), a novel framework designed to master this intricate reasoning style. VLM-R^3 is trained using a distinctive strategy that combines cold-start finetuning on our VLIR dataset with a novel Region-Conditioned Reinforcement Policy Optimization (R-GRPO). This empowers VLM-R^3 to learn when and where to look within an image, how to process the localized visual evidence (e.g., by cropping or requesting enhancement), and how to integrate this dynamically acquired information into its evolving reasoning chain. Our extensive experiments on diverse multimodal reasoning benchmarks, including MME [14], ScienceQA [30] and MathVista [29], demonstrate that VLM-R^3 significantly outperforms existing state-of-the-art models. In summary, our contributions are:

- The introduction of VLIR, the first benchmark dataset tailored for training and evaluating MLLMs on interleaved visual-textual CoT reasoning with explicit region-level interactions.

- The proposal of VLM-R^3, a novel MLLM framework, and its associated R-GRPO training strategy, which enables dynamic visual region localization and evidence integration within the reasoning process.
- Comprehensive empirical validation showing that VLM-R^3 achieves superior performance on challenging multimodal reasoning tasks, setting a new benchmark for fine-grained, visually-grounded inference.

2 Related Work

2.1 Large Language Model Reasoning

Reasoning in Large Language Models [49, 65, 63, 18] evolved substantially with Chain of Thought (CoT) prompting [48, 55, 23, 54, 34, 40], which enables models to break down complex problems into intermediate steps, mimicking human reasoning. This foundational approach has expanded to include diverse structures like program-of-thoughts [10], table-of-thoughts [19], and tree-of-thoughts [60], each offering unique advantages for different reasoning scenarios. Recent advances include OpenAI's O1 [36], which combines reinforcement learning [38, 43, 16] with CoT to optimize decision-making without external guidance, and DeepSeek R1 [12], which employs pure reinforcement learning through Group Relative Policy Optimization (GRPO) [45] to enable autonomous evolution of reasoning capabilities while incorporating rule-based rewards that significantly improve performance across complex reasoning tasks.

2.2 Multi-modal Large Language Model Reasoning

Multi-modal Large Language Model reasoning research [64, 56, 42, 33, 39, 28, 27] has emerged following the success of text-only reasoning models [36, 6, 12, 51], focusing on both effective multi-modal chain-of-thought structures [57, 52, 50, 20] and high-quality training data construction methods [13, 46, 4]. Mainstream approaches have adapted text-based reasoning paradigms to multi-modal contexts, as seen in Virgo [13], which demonstrated that text-only reasoning data can activate certain multi-modal reasoning capabilities, and more structured frameworks like LLaVA-CoT's [57] four-stage reasoning process and MM-Verify's [50] verification-enhanced approach. However, these methods largely inherit reasoning paradigms from text-only models without adequately addressing visual information processing, leading to limitations in visually-intensive reasoning tasks.

3 Method

We propose a novel framework, VLM-R^3, designed to perform visuo-lingual interleaved reasoning with region grounding. This section details the components of our approach, including the construction of the Visuo-Lingual Interleaved Rationale (VLIR) dataset used for cold-start supervised fine-tuning, the interactive inference pipeline enabling dynamic visual grounding, and the Region-Conditioned Reinforcement Policy Optimization (R-GRPO) strategy employed to enhance reasoning capabilities.

3.1 Visuo-Lingual Interleaved Rationale (VLIR) Dataset

Prior work, such as Visual CoT [44], introduced the concept of incorporating visual grounding (specifically bounding boxes) into reasoning chains. However, these methods typically suffer from several limitations: (1) They often lack explicit linguistic reasoning steps interleaved with visual actions. (2) The visual grounding actions (e.g., cropping based on bounding boxes) are predefined or manually specified, rather than being dynamically generated by the model. (3) They are often restricted to a limited number of visual interactions, typically a single bounding box selection before providing a final answer, lacking the flexibility for multi-step visual querying. To address these limitations and cultivate the ability for models to autonomously and flexibly perform iterative visual retrieval and cropping based on their ongoing reasoning, we introduce the **Visuo-Lingual Interleaved Rationale (VLIR)** dataset. This dataset is specifically curated to provide rich, interleaved sequences of textual reasoning steps interspersed with explicit visual grounding actions and the corresponding cropped visual evidence.

3.1.1 Data Construction

The construction of the VLIR dataset focuses on scenarios that necessitate fine-grained spatial understanding and precise utilization of visual cues. We select data from a diverse set of existing benchmarks to cover a wide range of visual reasoning challenges:

- **Text/Document Understanding:** TextVQA [47], DocVQA [32] for tasks requiring OCR and document structure understanding.
- **General Visual Question Answering:** GQA [17] for complex multistep reasoning over visual scenes.
- **Chart and Infographic Interpretation:** InfographicsVQA [31] for understanding structured visual data.
- **Spatial Relation Reasoning:** VSR [25] for tasks focused on identifying and reasoning about spatial relationships between objects.

We leverage the advanced capabilities of powerful MLLMs, such as Qwen2.5-VL 72B [8], through sophisticated prompt engineering to generate interleaved image-text reasoning chains for data points from benchmarks like GQA and TextVQA, which represent real-world question answering scenarios. We then employ a rejection sampling strategy on the generated samples, filtering for those that align with the ground-truth answers.

For tasks where direct prompt engineering on the original image-question pair is less effective, particularly those involving detailed OCR or tabular data interpretation (e.g., data underlying Visual CoT [44]), we utilize GPT-4o [35] with tailored prompts that incorporate the metadata provided by the source dataset (e.g., the initial bounding boxes from Visual CoT). This allows us to generate detailed, step-by-step interleaved rationales within these challenging domains.

3.1.2 Data Filtering

To ensure the quality and relevance of the interleaved rationales generated, we apply a rigorous filtering process based on the following criteria:

1. **Semantic Unit Validity of Regions:** Each proposed bounding box must enclose a complete and semantically meaningful visual unit (e.g., a recognizable object, a block of text, or a distinct part of a chart). To automate this, we utilize a smaller VLM and prompt it with the cropped image corresponding to the proposed bbox, asking it to confirm the presence and identity of a recognizable entity ("Can you identify what is in this image (a specific object or piece of text)? Respond with yes/no."). Samples in which the VLM fails to confirm a meaningful semantic unit are rejected.
2. **Logical Coherence and Non-Redundancy of Reasoning:** The generated textual reasoning steps must be logically sound, progressive, and directly contribute to arriving at the final answer, avoiding spurious or redundant text. We employ a powerful text-only LLM, such as DeepSeek V3 [24], through prompt engineering to evaluate the logical flow and relevance of the text rationale preceding each visual interaction and the overall reasoning path. Samples with illogical or padded reasoning are rejected.

3.2 Interactive Inference Pipeline

The VLM-R^3 model executes reasoning through an interactive pipeline that enables the model to dynamically select and incorporate visual information during its inference process.

The interaction is initiated by providing the VLM-R^3 with a system instruction that defines the reasoning task and the available visual interaction tool. This prompt includes directives such as

```
You need to first think about the reasoning process in your mind, and then
provide the answer. When thinking, you should call the "crop" tool (format:
{"bbox_2d": [x1, y1, x2, y2]}) to focus on the key areas in the image. The
reasoning process and the answer are included in the <think> </think> and
<answer> </answer> tags respectively.
```

When the model generates a string that matches the specified JSON format, the pipeline intercepts the output. The system parses the coordinates $[x1, y1, x2, y2]$ and performs a cropping operation on the original input image. The resulting cropped image is then zoomed in and encoded into visual tokens and appended to the model's input sequence, effectively providing the model with the requested visual detail as a new context. Following the injection of the cropped image, the model resumes generation, which may involve generating further text or issuing additional "Crop" commands. This interactive loop continues until the model generates the final answer, at which point the process terminates. This pipeline structure allows VLM-R^3 to perform multi-step, adaptive visual grounding guided by its evolving textual reasoning.

3.3 Region-Conditioned Reinforcement Policy Optimization (R-GRPO)

Standard supervised learning on fixed trajectories struggles to optimize the complex state-dependent policy of deciding *when* and *where* to acquire visual information. Our approach, Region-Conditioned Reinforcement Policy Optimization (R-GRPO), adapts a policy optimization framework, building upon Group Relative Policy Optimization (GRPO) [45]. The "Region-Conditioned" aspect implies that π_θ is explicitly conditioned on the visual state, including dynamically incorporated regional evidence.

To estimate the advantage of each reasoning trajectory, we normalize its reward relative to the group as follow:

$$\hat{A}^i = \frac{r^i - \text{mean}(\{r^1, r^2, ..., r^M\})}{\text{std}(\{r^1, r^2, ..., r^M\})} \tag{1}$$

Here, r^i is the total reward for the i-th trajectory in a group of M trajectories, and $\hat{A}^i$ serves as a form of advantage function relative to the group performance.

A critical adaptation in R-GRPO concerns the computation of the policy gradient and the actions considered in the objective. In our interleaved image-text sequences, some tokens are generated by the model (textual reasoning, bbox commands), while others (the representations of cropped images) are injected by the environment. The policy gradient should only optimize the likelihood of actions generated by the model. Therefore, when calculating the gradient of $\log \pi_\theta(a_t|s_t)$, we apply a mask: the gradient is computed only for tokens a_t that are text tokens or bounding box command tokens, masking out gradients for tokens corresponding to injected image regions. Conceptually, the sum of actions $\mathcal{A}_s$ in the loss primarily considers the probabilities of generating valid text tokens and bounding box commands, weighted by their advantage. The injected image tokens influence the state s_{t+1} but are not actions a_t for which we compute a policy gradient.

Following this, we optimize the policy model π_θ with the loss function defined as:

$$\mathcal{L}_{\text{GRPO}} = -\mathbb{E}_{Q \in D_S} \left[\sum_{i=1}^{M} \frac{\pi_\theta(c^i|Q)}{\pi_\theta(c^i|Q)|_{\text{no grad}}} \hat{A}^i - \beta D_{KL}(\pi_\theta || \pi_{\text{ref}}) \right] \tag{2}$$

where D_S is the dataset of question-state pairs, Q represents a specific question and current visual state, c^i is the sequence of generated tokens for the i-th trajectory given Q, and β is a coefficient for the KL divergence term. The first term in the sum uses the normalized reward $\hat{A}^i$ to weight the likelihood of the generated sequence, encouraging sequences with higher relative rewards.

The KL divergence between the policy model and the reference model is estimated as in [45]:

$$D_{KL}(\pi_\theta || \pi_{\text{ref}}) = \frac{\pi_{\text{ref}}(c^i|Q)}{\pi_\theta(c^i|Q)} - \log \frac{\pi_{\text{ref}}(c^i|Q)}{\pi_\theta(c^i|Q)} - 1 \tag{3}$$

The total reward r^i for a trajectory is a sum of several components designed to encourage the desired VLM-R^3 behaviors:

1. **Accuracy Reward (r_{acc}):** A sparse, terminal reward (1 for correct final answer, 0 otherwise).
2. **Format Adherence Reward (r_{format}):** A terminal reward (1 for correct <answer> tag format, 0 otherwise).
3. **Region Validity Reward (r_{valid}):** An intermediate reward (0.5) for each syntactically correct and non-redundant bounding box command generated, capped at 0.5 per episode.

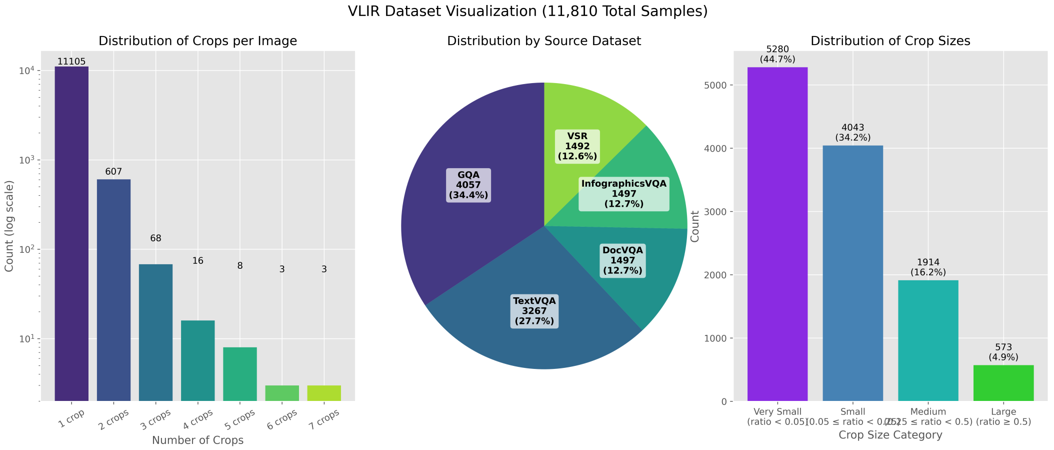

Figure 2: Distribution of the VLIR dataset: (a) number of crops per image, (b) samples across different source datasets, and (c) categorization of crops based on relative size.

4. **Reasoning Length Reward (r_{length}):** A small intermediate reward (0.001 per character) for generating reasoning steps, capped at 0.25 per episode.

By optimizing this objective, R-GRPO encourages the VLM to learn a policy that not only leads to correct final answers but also involves generating logical textual reasoning and strategically gathering the necessary visual evidence.

4 Experiments

4.1 Experiment Setting

We covers six public benchmarks. General vision–language understanding is measured on MME [14] and MMMU[62]; complex mathematical reasoning on MathVista [29] and MathVision [53]; scientific question answering on ScienceQA [30]; and document understanding on DocQA [32]. We also assess hallucination rates with HallucinationBench[15]. We evaluate our method against three categories of multimodal models. The first category consists of open-source baselines without explicit reasoning capability, including Qwen2.5-VL 7B [8] (also used as our primary baseline), InternVL2.5-8B [11], and LLaVA-Next 8B [21]. The second category comprises closed-source non-reasoning systems, represented by Gemini-2 Flash [1] and GPT-4o [35]. The third category contains models equipped with dedicated reasoning modules, namely LLaVA-CoT 11B [57] , Mulberry-Qwen2VL 7B [59], R1-onevision 7B [58]. To probe the upper bound of performance, we also compare our results with two larger closed-source models o1 [36].

4.2 Dataset Details

Our supervised fine-tuning experiments used the VLIR dataset, which comprises 11,810 samples in total. As shown in figure 2, the distribution of crops per image exhibits considerable variation: 11,105 images contain a single crop, 607 images feature two crops, 68 images have three crops, 16 images include four crops, 8 images contain five crops, and 6 images have six or seven crops (3 each). These samples are drawn from five distinct source datasets: GQA (4,057 samples), TextVQA (3,267 samples), DocVQA (1,497 samples), InfographicsVQA (1,497 samples), and VSR (1,492 samples). We categorize the crops based on their relative size, defined as the ratio of the bounding box area to the total image area: "very small" (ratio < 0.05) accounts for 5,280 crops; "small" (0.05 $\leq$ ratio < 0.25) comprises 4,043 crops; "medium" (0.25 $\leq$ ratio < 0.5) includes 1,914 crops; and "large" (ratio $\geq$ 0.5) consists of 573 crops.

4.3 Main Result

Our VLM-R^3 model, built upon the Qwen2.5-VL 7B architecture, consistently outperforms its base model across all benchmarks, with particularly significant gains in domains requiring precise

Model	Params	Benchmarks						
		MathVista	MathVision	MMMU	MME	ScienceQA	DocVQA	HallusionBench
Closed-Source Non-Reasoning MLLMs								
Gemini-2 Flash	-	73.1	41.3	71.7	-	-	92.1	-
GPT-4o	-	63.8	30.4	70.3	2328	66.2	91.1	56.2
Larger Closed-Source Models								
o1	-	71.8	63.2	77.6	-	-	81.6	-
Open-Source Non-Reasoning MLLMs								
InternVL2.5	8B	58.3	17.1	51.8	2210	-	-	-
LLaVA-Next	8B	37.5	-	41.7	1957	72.8	-	-
Open-Source Reasoning MLLMs								
LLaVA-CoT	11B	54.8	-	-	-	-	-	47.8
R1-onevision	7B	64.1	29.9	-	-	-	-	-
Vision-R1	7B	73.5	-	-	2190	-	-	49.5
Mulberry	7B	63.1	-	55.0	-	-	-	54.1
Qwen2.5-VL	7B	68.2	25.1	58.6	2347	73.6	95.7	61.3
Ours	7B	70.4	**30.2**	**62.2**	**2432**	**87.9**	**96.8**	**62.0**

Table 1: Performance comparison of various multimodal models across different benchmarks. Our model (in **bold**) is compared against non-reasoning models (both open-source and closed-source) and reasoning-based MLLMs. The highest values in each column are highlighted with green background. Benchmarks cover mathematics (MathVista, MathVision), general commonsense (MMMU, MME), science (ScienceQA), document understanding (DocVQA), and hallucination assessment (HallusionBench).

Model Variant	**MathVista**	**MMMU**	**ScienceQA**	**DocVQA**	**Avg.**
Base Model (Qwen2.5-VL)	68.2	58.6	73.6	95.7	74.0
w/o Interleaved Chain-of-Thought	67.1 (↓3.3)	59.4 (↓2.8)	75.4 (↓12.5)	95.9 (↓0.9)	74.4 (↓4.9)
w/o VLIR Fine-tuning	65.8 (↓4.6)	57.0 (↓5.2)	72.2 (↓15.7)	93.3 (↓3.5)	72.1 (↓7.2)
w/o R-GRPO	69.7 (↓0.7)	60.8 (↓1.4)	84.6 (↓3.3)	96.1 (↓0.7)	77.8 (↓1.5)
Full VLM-R^3 (Ours)	**70.4**	**62.2**	**87.9**	**96.8**	**79.3**

Table 2: Ablation study on MathVista, MMMU, ScienceQA, and DocVQA benchmarks. We evaluate the contribution of each key component: Interleaved Chain-of-Thought, VLIR fine-tuning, and R-GRPO.

visual reasoning and fine-grained understanding. Specifically, we observe a 2.2% improvement on MathVista (70.4% vs. 68.2%) and a remarkable 5.1% improvement on MathVision (30.2% vs. 25.1%), highlighting our method's effectiveness in mathematical reasoning tasks that demand careful attention to visual details. The substantial performance gain of 14.33% on ScienceQA (87.90% vs. 73.57%) further demonstrates VLM-R^3's superior capability in scientific reasoning, where dynamic grounding of visual evidence is critical. When compared to other open-source reasoning-focused models like Vision-R1 and Mulberry, VLM-R^3 exhibits competitive performance on MathVista and surpasses Mulberry on HallusionBench (62.0% vs. 54.1%), indicating enhanced reliability in avoiding visual hallucinations. Our approach also narrows the gap with closed-source models like Gemini-2 Flash and o1, despite having significantly fewer parameters and being fully transparent in its architecture.

4.4 Ablation Study

To assess the contribution of each component in our VLM-R^3 framework, we conduct comprehensive ablation experiments across four representative benchmarks: MathVista, MMMU, ScienceQA, and DocVQA. These benchmarks were selected to evaluate our method across diverse reasoning domains, from mathematical visual reasoning to scientific knowledge application and document understanding. Table 2 summarizes our findings.

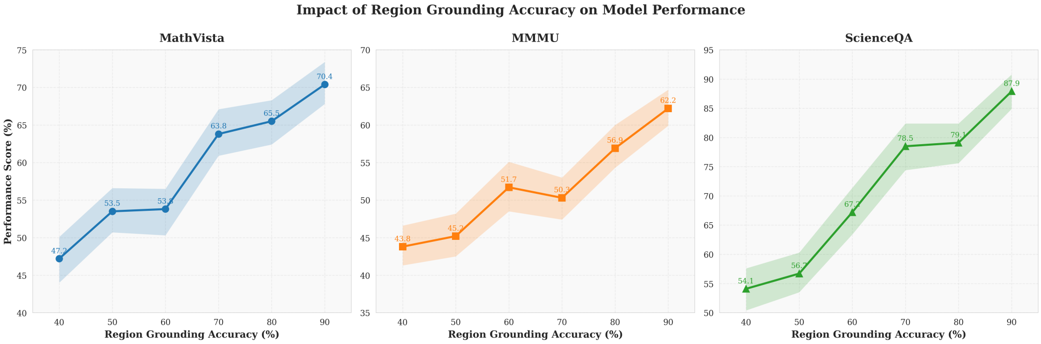

Figure 3: Impact of region grounding accuracy on model performance across three benchmarks. Each subplot shows the performance trajectory from 40% to 90% grounding accuracy with confidence intervals (shaded regions).

4.4.1 Effectiveness of Interleaved Chain-of-Thought

To isolate the impact of our interleaved reasoning approach, we conduct an experiment where we maintain the region localization capabilities (bounding boxes) but remove the associated region images from the reasoning chain. This variant relies solely on textual descriptions of identified regions without visually grounding each reasoning step. As shown in Table 2, removing the interleaved visual evidence leads to a consistent performance drop across all benchmarks, with particularly notable decreases on ScienceQA (-12.5%) and MMMU (-2.8%). This degradation is most pronounced in tasks requiring fine-grained visual understanding, such as scientific diagrams in ScienceQA, where purely textual descriptions of regions fail to capture crucial visual patterns and spatial relationships.

4.4.2 Effectiveness of Finetuning on VLIR

Our approach leverages the VLIR corpus to bootstrap the model's ability to identify informative regions and incorporate them into coherent reasoning chains. To evaluate the specific contribution of VLIR fine-tuning, we experiment with a variant that skips this initialization phase and proceeds directly to R-GRPO training. The results in Table 2 demonstrate that omitting VLIR fine-tuning leads to performance degradation across all benchmarks, with particularly significant decreases observed in ScienceQA (-15.7%) and MMMU (-5.2%). More critically, we observed that ablating VLIR fine-tuning impairs the model's instruction-following capabilities, leading to substantial deficiencies such as failures to adhere to required formatting conventions for bounding box specifications. This accounts for the substantial performance deterioration observed in our experimental results.

4.4.3 Effectiveness of R-GRPO

To assess the impact of our Region-Conditioned Reinforcement Policy Optimization (R-GRPO), we evaluate a variant that relies solely on supervised fine-tuning using the VLIR corpus without the subsequent reinforcement learning stage. This allows us to isolate the specific benefits of our reinforcement learning approach over purely supervised learning. The experimental results show that removing R-GRPO reduces performance in all benchmarks, with the highest decreases observed in ScienceQA (-3.28%) and MathVista (-0.7%). This suggests that while VLIR fine-tuning provides a strong foundation, the reinforcement learning stage is essential for optimizing the model's region selection and reasoning policies beyond what can be achieved through imitation learning alone.

4.5 Discussion

4.5.1 Impact of Region Grounding Accuracy on the Reasoning Chain

The quality of region grounding, represented by the accuracy of bounding boxes (bbox), plays a critical role in multimodal reasoning capabilities. Our analysis investigates how varying levels of grounding accuracy impact the performance of the VLM-R^3 model across multiple benchmarks. We systematically evaluated model performance by controlling grounding accuracy from 40% to 90% and measuring outcomes on three key benchmarks: ScienceQA, MathVista, and MMMU. Grounding accuracy was manipulated by randomly replacing or perturbing a controlled percentage of bounding

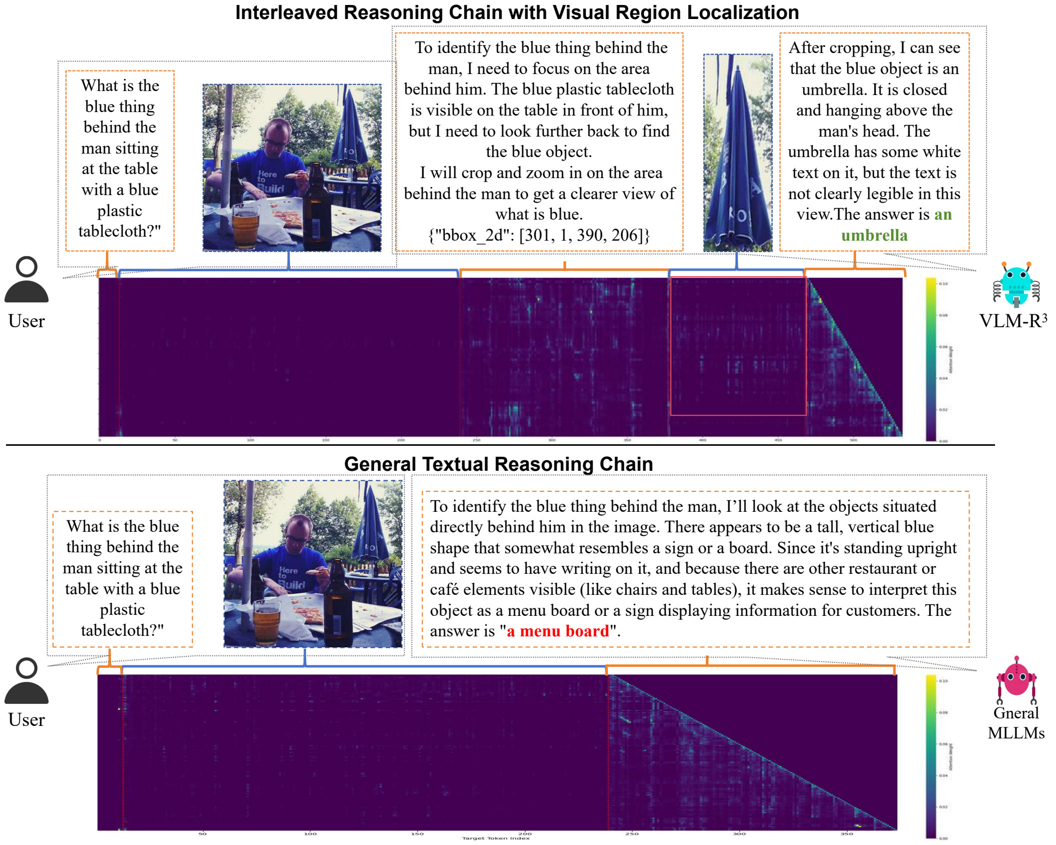

Interleaved Reasoning Chain with Visual Region Localization

What is the blue thing behind the man sitting at the table with a blue plastic tablecloth?"

To identify the blue thing behind the man, I need to focus on the area behind him. The blue plastic tablecloth is visible on the table in front of him, but I need to look further back to find the blue object.
I will crop and zoom in on the area behind the man to get a clearer view of what is blue.
{"bbox_2d": [301, 1, 390, 206]}

After cropping, I can see that the blue object is an umbrella. It is closed and hanging above the man's head. The umbrella has some white text on it, but the text is not clearly legible in this view.The answer is **an umbrella**

General Textual Reasoning Chain

What is the blue thing behind the man sitting at the table with a blue plastic tablecloth?"

To identify the blue thing behind the man, I'll look at the objects situated directly behind him in the image. There appears to be a tall, vertical blue shape that somewhat resembles a sign or a board. Since it's standing upright and seems to have writing on it, and because there are other restaurant or café elements visible (like chairs and tables), it makes sense to interpret this object as a menu board or a sign displaying information for customers. The answer is "**a menu board**".

Figure 4: Comparison of attention distribution patterns between the interleaved reasoning chain with visual region localization (top) and general textual reasoning chain (bottom).

boxes in the input. As shown in Figure 3, there is a clear positive correlation between region grounding accuracy and model performance across all three benchmarks. ScienceQA demonstrates the most substantial improvement, with performance increasing from 54.1% at 40% grounding accuracy to 87.9% at 90% grounding accuracy. MathVista shows a similar upward trend, rising from 47.9% to 70.4%, while MMMU exhibits more modest but consistent gains from 43.8% to 62.2%. These results underscore the fundamental importance of precise region grounding for effective multimodal reasoning, with higher-level reasoning tasks showing greater sensitivity to grounding quality.

4.5.2 Why is the Interleaved Reasoning Chain with Visual Region Localization Effective?

To understand the efficacy of our VLM-R^3 approach, we conducted a comparative analysis between the interleaved reasoning chain with visual region localization and traditional textual reasoning chains. Figure 4 visualizes the attention distribution patterns for both approaches when answering the same visual query. Our analysis reveals a critical insight: in traditional approaches where the image is positioned at the beginning of the sequence, attention to visual information diminishes significantly as the reasoning chain progresses. As shown in the lower portion of Figure 4, general MLMs tend to make incorrect inferences (identifying a "menu board" instead of an umbrella) as they lose visual context during extended reasoning. In contrast, VLM-R^3 maintains persistent visual attention throughout the reasoning process by dynamically localizing and incorporating relevant visual regions. The attention heatmap demonstrates that tokens generated later in the reasoning process maintain strong attention connections to the cropped visual regions. This region-specific attention enables the model to correctly identify the blue object as an umbrella by explicitly focusing on the area behind the person, cropping it for detailed examination, and making accurate observations about its features.

5 Conclusion

This paper introduced VLM-R^3, a novel framework enabling MLLMs to perform dynamic visual reasoning through region recognition, reasoning, and refinement. By integrating our custom VLIR dataset and Region-Conditioned Reinforcement Policy Optimization (R-GRPO), we demonstrated that interleaved visual-textual chains-of-thought significantly outperform traditional approaches. VLM-R^3 achieves state-of-the-art results across multiple benchmarks, particularly excelling in tasks requiring fine-grained spatial reasoning and visual evidence integration. Our work opens promising directions for developing more sophisticated visually-grounded reasoning systems that can adaptively focus on relevant regions during multi-step inference processes.

References

[1] Gemini 2.5: Our most intelligent ai model, 2024. https://deepmind.google/technologies/gemini/.

[2] Introducing openai o3 and o4-mini, 2024. https://openai.com/index/introducing-o3-and-o4-mini/.

[3] Qvq: To see the world with wisdom, 2024. https://qwenlm.github.io/blog/qvq-72b-preview/.

[4] Seekworld: Geolocation is a natural rl task for o3-like visual clue-tracking reasoning, 2025. https://huggingface.co/datasets/TheEighthDay/SeekWorld.

[5] Jean-Baptiste Alayrac, Jeff Donahue, Pauline Luc, et al. Flamingo: a visual language model for few-shot learning. In *NeurIPS*, volume 35, 2022.

[6] Gemini Team Google Rohan Anil, Sebastian Borgeaud, Yonghui Wu, Jean-Baptiste Alayrac, Jiahui Yu, Radu Soricut, and Johan Schalkwyk... Gemini: A family of highly capable multimodal models. *ArXiv*, abs/2312.11805, 2023.

[7] Jinze Bai, Shuai Bai, Shusheng Yang, Shijie Wang, Sinan Tan, Peng Wang, Junyang Lin, Chang Zhou, and Jingren Zhou. Qwen-vl: A frontier large vision-language model with versatile abilities. *ArXiv*, abs/2308.12966, 2023.

[8] Shuai Bai, Keqin Chen, Xuejing Liu, Jialin Wang, Wenbin Ge, Sibo Song, Kai Dang, Peng Wang, Shijie Wang, Jun Tang, Humen Zhong, Yuanzhi Zhu, Mingkun Yang, Zhaohai Li, Jianqiang Wan, Pengfei Wang, Wei Ding, Zheren Fu, Yiheng Xu, Jiabo Ye, Xi Zhang, Tianbao Xie, Zesen Cheng, Hang Zhang, Zhibo Yang, Haiyang Xu, and Junyang Lin. Qwen2.5-vl technical report. *ArXiv*, abs/2502.13923, 2025.

[9] Qiguang Chen, Libo Qin, Jin Zhang, Zhi Chen, Xiao Xu, and Wanxiang Che. M^{3}cot: A novel benchmark for multi-domain multi-step multi-modal chain-of-thought, 2024.

[10] Wenhu Chen, Xueguang Ma, Xinyi Wang, and William W. Cohen. Program of thoughts prompting: Disentangling computation from reasoning for numerical reasoning tasks. *Trans. Mach. Learn. Res.*, 2023, 2022.

[11] Zhe Chen, Weiyun Wang, Yue Cao, Yangzhou Liu, Zhangwei Gao, Erfei Cui, Jinguo Zhu, Shenglong Ye, Hao Tian, Zhaoyang Liu, Lixin Gu, Xuehui Wang, Qingyun Li, Yimin Ren, Zixuan Chen, Jiapeng Luo, Jiahao Wang, Tan Jiang, Bo Wang, Conghui He, Botian Shi, Xingcheng Zhang, Han Lv, Yi Wang, Wenqi Shao, Pei Chu, Zhongying Tu, Tong He, Zhiyong Wu, Huipeng Deng, Jiaye Ge, Kai Chen, Kaipeng Zhang, Limin Wang, Min Dou, Lewei Lu, Xizhou Zhu, Tong Lu, Dahua Lin, Yu Qiao, Jifeng Dai, and Wenhai Wang. Expanding performance boundaries of open-source multimodal models with model, data, and test-time scaling, 2025.

[12] DeepSeek-AI, Daya Guo, Dejian Yang, Haowei Zhang, Jun-Mei Song, Ruoyu Zhang, Runxin Xu, Qihao Zhu, Shirong Ma, Peiyi Wang, Xiaoling Bi, Xiaokang Zhang, Xingkai Yu, Yu Wu, Z. F. Wu, Zhibin Gou, Zhihong Shao, Zhuoshu Li, Ziyi Gao, Aixin Liu, Bing Xue, Bing-Li Wang, Bochao Wu, Bei Feng, Chengda Lu, Chenggang Zhao, Chengqi Deng, Chenyu Zhang, Chong Ruan, Damai Dai, Deli Chen, Dong-Li Ji, Erhang Li, Fangyun Lin, Fucong Dai, Fuli Luo, Guangbo Hao, Guanting Chen, Guowei Li, H. Zhang, Han Bao, Hanwei Xu, Haocheng

Wang, Honghui Ding, Huajian Xin, Huazuo Gao, Hui Qu, Hui Li, Jianzhong Guo, Jiashi Li, Jiawei Wang, Jingchang Chen, Jingyang Yuan, Junjie Qiu, Junlong Li, Jiong Cai, Jiaqi Ni, Jian Liang, Jin Chen, Kai Dong, Kai Hu, Kaige Gao, Kang Guan, Kexin Huang, Kuai Yu, Lean Wang, Lecong Zhang, Liang Zhao, Litong Wang, Liyue Zhang, Lei Xu, Leyi Xia, Mingchuan Zhang, Minghua Zhang, M. Tang, Meng Li, Miaojun Wang, Mingming Li, Ning Tian, Panpan Huang, Peng Zhang, Qiancheng Wang, Qinyu Chen, Qiushi Du, Ruiqi Ge, Ruisong Zhang, Ruizhe Pan, Runji Wang, R. J. Chen, Ruiqi Jin, Ruyi Chen, Shanghao Lu, Shangyan Zhou, Shanhuang Chen, Shengfeng Ye, Shiyu Wang, Shuiping Yu, Shunfeng Zhou, Shuting Pan, S. S. Li, Shuang Zhou, Shao-Kang Wu, Tao Yun, Tian Pei, Tianyu Sun, T. Wang, Wangding Zeng, Wanjia Zhao, Wen Liu, Wenfeng Liang, Wenjun Gao, Wen-Xia Yu, Wentao Zhang, W. L. Xiao, Wei An, Xiaodong Liu, Xiaohan Wang, Xiaokang Chen, Xiaotao Nie, Xin Cheng, Xin Liu, Xin Xie, Xingchao Liu, Xinyu Yang, Xinyuan Li, Xuecheng Su, Xuheng Lin, X. Q. Li, Xiangyu Jin, Xi-Cheng Shen, Xiaosha Chen, Xiaowen Sun, Xiaoxiang Wang, Xinnan Song, Xinyi Zhou, Xianzu Wang, Xinxia Shan, Y. K. Li, Y. Q. Wang, Y. X. Wei, Yang Zhang, Yanhong Xu, Yao Li, Yao Zhao, Yaofeng Sun, Yaohui Wang, Yi Yu, Yichao Zhang, Yifan Shi, Yi Xiong, Ying He, Yishi Piao, Yisong Wang, Yixuan Tan, Yiyang Ma, Yiyuan Liu, Yongqiang Guo, Yuan Ou, Yuduan Wang, Yue Gong, Yu-Jing Zou, Yujia He, Yunfan Xiong, Yu-Wei Luo, Yu mei You, Yuxuan Liu, Yuyang Zhou, Y. X. Zhu, Yanping Huang, Yao Li, Yi Zheng, Yuchen Zhu, Yunxiang Ma, Ying Tang, Yukun Zha, Yuting Yan, Zehui Ren, Zehui Ren, Zhangli Sha, Zhe Fu, Zhean Xu, Zhenda Xie, Zhen guo Zhang, Zhewen Hao, Zhicheng Ma, Zhigang Yan, Zhiyu Wu, Zihui Gu, Zijia Zhu, Zijun Liu, Zi-An Li, Ziwei Xie, Ziyang Song, Zizheng Pan, Zhen Huang, Zhipeng Xu, Zhongyu Zhang, and Zhen Zhang. Deepseek-r1: Incentivizing reasoning capability in llms via reinforcement learning. *ArXiv*, abs/2501.12948, 2025.

[13] Yifan Du, Zikang Liu, Yifan Li, Wayne Xin Zhao, Yuqi Huo, Bingning Wang, Weipeng Chen, Zheng Liu, Zhongyuan Wang, and Ji-Rong Wen. Virgo: A preliminary exploration on reproducing o1-like mllm, 2025.

[14] Chaoyou Fu, Peixian Chen, Yunhang Shen, Yulei Qin, Mengdan Zhang, Xu Lin, Zhenyu Qiu, Wei Lin, Jinrui Yang, Xiawu Zheng, et al. Mme: A comprehensive evaluation benchmark for multimodal large language models. *arXiv preprint arXiv:2306.13394*, 2023.

[15] Tianrui Guan, Fuxiao Liu, Xiyang Wu, Ruiqi Xian, Zongxia Li, Xiaoyu Liu, Xijun Wang, Lichang Chen, Furong Huang, Yaser Yacoob, Dinesh Manocha, and Tianyi Zhou. Hallusionbench: An advanced diagnostic suite for entangled language hallucination and visual illusion in large vision-language models, 2024.

[16] Jian Hu. Reinforce++: A simple and efficient approach for aligning large language models. *arXiv preprint arXiv:2501.03262*, 2025.

[17] Drew A Hudson and Christopher D Manning. Gqa: A new dataset for real-world visual reasoning and compositional question answering. In *Proceedings of the IEEE/CVF conference on computer vision and pattern recognition*, pages 6700–6709, 2019.

[18] Shima Imani, Liang Du, and Harsh Shrivastava. Mathprompter: Mathematical reasoning using large language models. *arXiv preprint arXiv:2303.05398*, 2023.

[19] Ziqi Jin and Wei Lu. Tab-cot: Zero-shot tabular chain of thought. In *Annual Meeting of the Association for Computational Linguistics*, 2023.

[20] Chengzu Li, Wenshan Wu, Huanyu Zhang, Yan Xia, Shaoguang Mao, Li Dong, Ivan Vulić, and Furu Wei. Imagine while reasoning in space: Multimodal visualization-of-thought, 2025.

[21] Feng Li, Renrui Zhang, Hao Zhang, Yuanhan Zhang, Bo Li, Wei Li, Zejun Ma, and Chunyuan Li. Llava-next-interleave: Tackling multi-image, video, and 3d in large multimodal models, 2024.

[22] Junnan Li, Dongxu Li, Silvio Savarese, et al. Blip-2: Bootstrapping language-image pre-training with frozen image encoders and large language models. In *ICML*, 2023.

[23] Hunter Lightman, Vineet Kosaraju, Yura Burda, Harri Edwards, Bowen Baker, Teddy Lee, Jan Leike, John Schulman, Ilya Sutskever, and Karl Cobbe. Let's verify step by step, 2023.

[24] Aixin Liu, Bei Feng, Bing Xue, Bingxuan Wang, Bochao Wu, Chengda Lu, Chenggang Zhao, Chengqi Deng, Chenyu Zhang, Chong Ruan, et al. Deepseek-v3 technical report. *arXiv preprint arXiv:2412.19437*, 2024.

[25] Fangyu Liu, Guy Emerson, and Nigel Collier. Visual spatial reasoning, 2023.

[26] Haotian Liu, Chunyuan Li, Yuheng Li, et al. Improved baselines with visual instruction tuning. *arXiv preprint arXiv:2310.03744*, 2023.

[27] Yuqi Liu, Bohao Peng, Zhisheng Zhong, Zihao Yue, Fanbin Lu, Bei Yu, and Jiaya Jia. Seg-zero: Reasoning-chain guided segmentation via cognitive reinforcement, 2025.

[28] Ziyu Liu, Zeyi Sun, Yuhang Zang, Xiaoyi Dong, Yuhang Cao, Haodong Duan, Dahua Lin, and Jiaqi Wang. Visual-rft: Visual reinforcement fine-tuning, 2025.

[29] Pan Lu, Hritik Bansal, Tony Xia, Jiacheng Liu, Chunyuan Li, Hannaneh Hajishirzi, Hao Cheng, Kai-Wei Chang, Michel Galley, and Jianfeng Gao. Mathvista: Evaluating mathematical reasoning of foundation models in visual contexts, 2024.

[30] Pan Lu, Swaroop Mishra, Tony Xia, Liang Qiu, Kai-Wei Chang, Song-Chun Zhu, Oyvind Tafjord, Peter Clark, and Ashwin Kalyan. Learn to explain: Multimodal reasoning via thought chains for science question answering, 2022.

[31] Minesh Mathew, Viraj Bagal, Rubèn Pérez Tito, Dimosthenis Karatzas, Ernest Valveny, and C. V Jawahar. Infographicvqa, 2021.

[32] Minesh Mathew, Dimosthenis Karatzas, and C. V. Jawahar. Docvqa: A dataset for vqa on document images, 2021.

[33] Minheng Ni, Yutao Fan, Lei Zhang, and Wangmeng Zuo. Visual-o1: Understanding ambiguous instructions via multi-modal multi-turn chain-of-thoughts reasoning. *arXiv preprint arXiv:2410.03321*, 2024.

[34] Xuefei Ning, Zinan Lin, Zixuan Zhou, Zifu Wang, Huazhong Yang, and Yu Wang. Skeleton-of-thought: Prompting llms for efficient parallel generation. *arXiv preprint arXiv:2307.15337*, 2023.

[35] OpenAI, :, Aaron Hurst, Adam Lerer, Adam P. Goucher, Adam Perelman, Aditya Ramesh, Aidan Clark, AJ Ostrow, Akila Welihinda, Alan Hayes, Alec Radford, Aleksander Mądry, Alex Baker-Whitcomb, Alex Beutel, Alex Borzunov, Alex Carney, Alex Chow, Alex Kirillov, Alex Nichol, Alex Paino, Alex Renzin, Alex Tachard Passos, Alexander Kirillov, Alexi Christakis, Alexis Conneau, Ali Kamali, Allan Jabri, Allison Moyer, Allison Tam, Amadou Crookes, Amin Tootoochian, Amin Tootoonchian, Ananya Kumar, Andrea Vallone, Andrej Karpathy, Andrew Braunstein, Andrew Cann, Andrew Codispoti, Andrew Galu, Andrew Kondrich, Andrew Tulloch, Andrey Mishchenko, Angela Baek, Angela Jiang, Antoine Pelisse, Antonia Woodford, Anuj Gosalia, Arka Dhar, Ashley Pantuliano, Avi Nayak, Avital Oliver, Barret Zoph, Behrooz Ghorbani, Ben Leimberger, Ben Rossen, Ben Sokolowsky, Ben Wang, Benjamin Zweig, Beth Hoover, Blake Samic, Bob McGrew, Bobby Spero, Bogo Giertler, Bowen Cheng, Brad Lightcap, Brandon Walkin, Brendan Quinn, Brian Guarraci, Brian Hsu, Bright Kellogg, Brydon Eastman, Camillo Lugaresi, Carroll Wainwright, Cary Bassin, Cary Hudson, Casey Chu, Chad Nelson, Chak Li, Chan Jun Shern, Channing Conger, Charlotte Barette, Chelsea Voss, Chen Ding, Cheng Lu, Chong Zhang, Chris Beaumont, Chris Hallacy, Chris Koch, Christian Gibson, Christina Kim, Christine Choi, Christine McLeavey, Christopher Hesse, Claudia Fischer, Clemens Winter, Coley Czarnecki, Colin Jarvis, Colin Wei, Constantin Koumouzelis, Dane Sherburn, Daniel Kappler, Daniel Levin, Daniel Levy, David Carr, David Farhi, David Mely, David Robinson, David Sasaki, Denny Jin, Dev Valladares, Dimitris Tsipras, Doug Li, Duc Phong Nguyen, Duncan Findlay, Edede Oiwoh, Edmund Wong, Ehsan Asdar, Elizabeth Proehl, Elizabeth Yang, Eric Antonow, Eric Kramer, Eric Peterson, Eric Sigler, Eric Wallace, Eugene Brevdo, Evan Mays, Farzad Khorasani, Felipe Petroski Such, Filippo Raso, Francis Zhang, Fred von Lohmann, Freddie Sulit, Gabriel Goh, Gene Oden, Geoff Salmon, Giulio Starace, Greg Brockman, Hadi Salman, Haiming Bao, Haitang Hu, Hannah Wong, Haoyu Wang, Heather Schmidt, Heather Whitney, Heewoo Jun, Hendrik Kirchner, Henrique Ponde de Oliveira Pinto, Hongyu Ren, Huiwen Chang, Hyung Won Chung, Ian Kivlichan, Ian O'Connell, Ian O'Connell, Ian Osband, Ian

Silber, Ian Sohl, Ibrahim Okuyucu, Ikai Lan, Ilya Kostrikov, Ilya Sutskever, Ingmar Kanitscheider, Ishaan Gulrajani, Jacob Coxon, Jacob Menick, Jakub Pachocki, James Aung, James Betker, James Crooks, James Lennon, Jamie Kiros, Jan Leike, Jane Park, Jason Kwon, Jason Phang, Jason Teplitz, Jason Wei, Jason Wolfe, Jay Chen, Jeff Harris, Jenia Varavva, Jessica Gan Lee, Jessica Shieh, Ji Lin, Jiahui Yu, Jiayi Weng, Jie Tang, Jieqi Yu, Joanne Jang, Joaquin Quinonero Candela, Joe Beutler, Joe Landers, Joel Parish, Johannes Heidecke, John Schulman, Jonathan Lachman, Jonathan McKay, Jonathan Uesato, Jonathan Ward, Jong Wook Kim, Joost Huizinga, Jordan Sitkin, Jos Kraaijeveld, Josh Gross, Josh Kaplan, Josh Snyder, Joshua Achiam, Joy Jiao, Joyce Lee, Juntang Zhuang, Justyn Harriman, Kai Fricke, Kai Hayashi, Karan Singhal, Katy Shi, Kavin Karthik, Kayla Wood, Kendra Rimbach, Kenny Hsu, Kenny Nguyen, Keren Gu-Lemberg, Kevin Button, Kevin Liu, Kiel Howe, Krithika Muthukumar, Kyle Luther, Lama Ahmad, Larry Kai, Lauren Itow, Lauren Workman, Leher Pathak, Leo Chen, Li Jing, Lia Guy, Liam Fedus, Liang Zhou, Lien Mamitsuka, Lilian Weng, Lindsay McCallum, Lindsey Held, Long Ouyang, Louis Feuvrier, Lu Zhang, Lukas Kondraciuk, Lukasz Kaiser, Luke Hewitt, Luke Metz, Lyric Doshi, Mada Aflak, Maddie Simens, Madelaine Boyd, Madeleine Thompson, Marat Dukhan, Mark Chen, Mark Gray, Mark Hudnall, Marvin Zhang, Marwan Aljubeh, Mateusz Litwin, Matthew Zeng, Max Johnson, Maya Shetty, Mayank Gupta, Meghan Shah, Mehmet Yatbaz, Meng Jia Yang, Mengchao Zhong, Mia Glaese, Mianna Chen, Michael Janner, Michael Lampe, Michael Petrov, Michael Wu, Michele Wang, Michelle Fradin, Michelle Pokrass, Miguel Castro, Miguel Oom Temudo de Castro, Mikhail Pavlov, Miles Brundage, Miles Wang, Minal Khan, Mira Murati, Mo Bavarian, Molly Lin, Murat Yesildal, Nacho Soto, Natalia Gimelshein, Natalie Cone, Natalie Staudacher, Natalie Summers, Natan LaFontaine, Neil Chowdhury, Nick Ryder, Nick Stathas, Nick Turley, Nik Tezak, Niko Felix, Nithanth Kudige, Nitish Keskar, Noah Deutsch, Noel Bundick, Nora Puckett, Ofir Nachum, Ola Okelola, Oleg Boiko, Oleg Murk, Oliver Jaffe, Olivia Watkins, Olivier Godement, Owen Campbell-Moore, Patrick Chao, Paul McMillan, Pavel Belov, Peng Su, Peter Bak, Peter Bakkum, Peter Deng, Peter Dolan, Peter Hoeschele, Peter Welinder, Phil Tillet, Philip Pronin, Philippe Tillet, Prafulla Dhariwal, Qiming Yuan, Rachel Dias, Rachel Lim, Rahul Arora, Rajan Troll, Randall Lin, Rapha Gontijo Lopes, Raul Puri, Reah Miyara, Reimar Leike, Renaud Gaubert, Reza Zamani, Ricky Wang, Rob Donnelly, Rob Honsby, Rocky Smith, Rohan Sahai, Rohit Ramchandani, Romain Huet, Rory Carmichael, Rowan Zellers, Roy Chen, Ruby Chen, Ruslan Nigmatullin, Ryan Cheu, Saachi Jain, Sam Altman, Sam Schoenholz, Sam Toizer, Samuel Miserendino, Sandhini Agarwal, Sara Culver, Scott Ethersmith, Scott Gray, Sean Grove, Sean Metzger, Shamez Hermani, Shantanu Jain, Shengjia Zhao, Sherwin Wu, Shino Jomoto, Shirong Wu, Shuaiqi, Xia, Sonia Phene, Spencer Papay, Srinivas Narayanan, Steve Coffey, Steve Lee, Stewart Hall, Suchir Balaji, Tal Broda, Tal Stramer, Tao Xu, Tarun Gogineni, Taya Christianson, Ted Sanders, Tejal Patwardhan, Thomas Cunninghman, Thomas Degry, Thomas Dimson, Thomas Raoux, Thomas Shadwell, Tianhao Zheng, Todd Underwood, Todor Markov, Toki Sherbakov, Tom Rubin, Tom Stasi, Tomer Kaftan, Tristan Heywood, Troy Peterson, Tyce Walters, Tyna Eloundou, Valerie Qi, Veit Moeller, Vinnie Monaco, Vishal Kuo, Vlad Fomenko, Wayne Chang, Weiyi Zheng, Wenda Zhou, Wesam Manassra, Will Sheu, Wojciech Zaremba, Yash Patil, Yilei Qian, Yongjik Kim, Youlong Cheng, Yu Zhang, Yuchen He, Yuchen Zhang, Yujia Jin, Yunxing Dai, and Yury Malkov. Gpt-4o system card, 2024.

[36] OpenAI, :, Aaron Jaech, Adam Kalai, Adam Lerer, Adam Richardson, Ahmed El-Kishky, Aiden Low, Alec Helyar, Aleksander Madry, Alex Beutel, Alex Carney, Alex Iftimie, Alex Karpenko, Alex Tachard Passos, Alexander Neitz, Alexander Prokofiev, Alexander Wei, Allison Tam, Ally Bennett, Ananya Kumar, Andre Saraiva, Andrea Vallone, Andrew Duberstein, Andrew Kondrich, Andrey Mishchenko, Andy Applebaum, Angela Jiang, Ashvin Nair, Barret Zoph, Behrooz Ghorbani, Ben Rossen, Benjamin Sokolowsky, Boaz Barak, Bob McGrew, Borys Minaiev, Botao Hao, Bowen Baker, Brandon Houghton, Brandon McKinzie, Brydon Eastman, Camillo Lugaresi, Cary Bassin, Cary Hudson, Chak Ming Li, Charles de Bourcy, Chelsea Voss, Chen Shen, Chong Zhang, Chris Koch, Chris Orsinger, Christopher Hesse, Claudia Fischer, Clive Chan, Dan Roberts, Daniel Kappler, Daniel Levy, Daniel Selsam, David Dohan, David Farhi, David Mely, David Robinson, Dimitris Tsipras, Doug Li, Dragos Oprica, Eben Freeman, Eddie Zhang, Edmund Wong, Elizabeth Proehl, Enoch Cheung, Eric Mitchell, Eric Wallace, Erik Ritter, Evan Mays, Fan Wang, Felipe Petroski Such, Filippo Raso, Florencia Leoni, Foivos Tsimpourlas, Francis Song, Fred von Lohmann, Freddie Sulit, Geoff Salmon, Giambattista Parascandolo, Gildas Chabot, Grace Zhao, Greg Brockman, Guillaume Leclerc,

Hadi Salman, Haiming Bao, Hao Sheng, Hart Andrin, Hessam Bagherinezhad, Hongyu Ren, Hunter Lightman, Hyung Won Chung, Ian Kivlichan, Ian O'Connell, Ian Osband, Ignasi Clavera Gilaberte, Ilge Akkaya, Ilya Kostrikov, Ilya Sutskever, Irina Kofman, Jakub Pachocki, James Lennon, Jason Wei, Jean Harb, Jerry Twore, Jiacheng Feng, Jiahui Yu, Jiayi Weng, Jie Tang, Jieqi Yu, Joaquin Quiñonero Candela, Joe Palermo, Joel Parish, Johannes Heidecke, John Hallman, John Rizzo, Jonathan Gordon, Jonathan Uesato, Jonathan Ward, Joost Huizinga, Julie Wang, Kai Chen, Kai Xiao, Karan Singhal, Karina Nguyen, Karl Cobbe, Katy Shi, Kayla Wood, Kendra Rimbach, Keren Gu-Lemberg, Kevin Liu, Kevin Lu, Kevin Stone, Kevin Yu, Lama Ahmad, Lauren Yang, Leo Liu, Leon Maksin, Leyton Ho, Liam Fedus, Lilian Weng, Linden Li, Lindsay McCallum, Lindsey Held, Lorenz Kuhn, Lukas Kondraciuk, Lukasz Kaiser, Luke Metz, Madelaine Boyd, Maja Trebacz, Manas Joglekar, Mark Chen, Marko Tintor, Mason Meyer, Matt Jones, Matt Kaufer, Max Schwarzer, Meghan Shah, Mehmet Yatbaz, Melody Y. Guan, Mengyuan Xu, Mengyuan Yan, Mia Glaese, Mianna Chen, Michael Lampe, Michael Malek, Michele Wang, Michelle Fradin, Mike McClay, Mikhail Pavlov, Miles Wang, Mingxuan Wang, Mira Murati, Mo Bavarian, Mostafa Rohaninejad, Nat McAleese, Neil Chowdhury, Neil Chowdhury, Nick Ryder, Nikolas Tezak, Noam Brown, Ofir Nachum, Oleg Boiko, Oleg Murk, Olivia Watkins, Patrick Chao, Paul Ashbourne, Pavel Izmailov, Peter Zhokhov, Rachel Dias, Rahul Arora, Randall Lin, Rapha Gontijo Lopes, Raz Gaon, Reah Miyara, Reimar Leike, Renny Hwang, Rhythm Garg, Robin Brown, Roshan James, Rui Shu, Ryan Cheu, Ryan Greene, Saachi Jain, Sam Altman, Sam Toizer, Sam Toyer, Samuel Miserendino, Sandhini Agarwal, Santiago Hernandez, Sasha Baker, Scott McKinney, Scottie Yan, Shengjia Zhao, Shengli Hu, Shibani Santurkar, Shraman Ray Chaudhuri, Shuyuan Zhang, Siyuan Fu, Spencer Papay, Steph Lin, Suchir Balaji, Suvansh Sanjeev, Szymon Sidor, Tal Broda, Aidan Clark, Tao Wang, Taylor Gordon, Ted Sanders, Tejal Patwardhan, Thibault Sottiaux, Thomas Degry, Thomas Dimson, Tianhao Zheng, Timur Garipov, Tom Stasi, Trapit Bansal, Trevor Creech, Troy Peterson, Tyna Eloundou, Valerie Qi, Vineet Kosaraju, Vinnie Monaco, Vitchyr Pong, Vlad Fomenko, Weiyi Zheng, Wenda Zhou, Wes McCabe, Wojciech Zaremba, Yann Dubois, Yinghai Lu, Yining Chen, Young Cha, Yu Bai, Yuchen He, Yuchen Zhang, Yunyun Wang, Zheng Shao, and Zhuohan Li. Openai o1 system card, 2024.

[37] OpenAI. Gpt-4v(ision) system card. `https://cdn.openai.com/papers/GPTV_System_Card.pdf`, 2023.

[38] Long Ouyang, Jeff Wu, Xu Jiang, Diogo Almeida, Carroll L. Wainwright, Pamela Mishkin, Chong Zhang, Sandhini Agarwal, Katarina Slama, Alex Ray, John Schulman, Jacob Hilton, Fraser Kelton, Luke Miller, Maddie Simens, Amanda Askell, Peter Welinder, Paul Christiano, Jan Leike, and Ryan Lowe. Training language models to follow instructions with human feedback, 2022.

[39] Yingzhe Peng, Gongrui Zhang, Miaosen Zhang, Zhiyuan You, Jie Liu, Qipeng Zhu, Kai Yang, Xingzhong Xu, Xin Geng, and Xu Yang. Lmm-r1: Empowering 3b lmms with strong reasoning abilities through two-stage rule-based rl, 2025.

[40] Zhenting Qi, Mingyuan Ma, Jiahang Xu, Li Lyna Zhang, Fan Yang, and Mao Yang. Mutual reasoning makes smaller llms stronger problem-solvers. *arXiv preprint arXiv:2408.06195*, 2024.

[41] Jeff Rasley, Samyam Rajbhandari, Olatunji Ruwase, and Yuxiong He. Deepspeed: System optimizations enable training deep learning models with over 100 billion parameters. In *Proceedings of the 26th ACM SIGKDD international conference on knowledge discovery & data mining*, pages 3505–3506, 2020.

[42] Daniel Rose, Vaishnavi Himakunthala, Andy Ouyang, Ryan He, Alex Mei, Yujie Lu, Michael Saxon, Chinmay Sonar, Diba Mirza, and William Yang Wang. Visual chain of thought: bridging logical gaps with multimodal infillings. *arXiv preprint arXiv:2305.02317*, 2023.

[43] John Schulman, Filip Wolski, Prafulla Dhariwal, Alec Radford, and Oleg Klimov. Proximal policy optimization algorithms. *arXiv preprint arXiv:1707.06347*, 2017.

[44] Hao Shao, Shengju Qian, Han Xiao, Guanglu Song, Zhuofan Zong, Letian Wang, Yu Liu, and Hongsheng Li. Visual cot: Advancing multi-modal language models with a comprehensive dataset and benchmark for chain-of-thought reasoning, 2024.

[45] Zhihong Shao, Peiyi Wang, Qihao Zhu, Runxin Xu, Junxiao Song, Xiao Bi, Haowei Zhang, Mingchuan Zhang, Y. K. Li, Y. Wu, and Daya Guo. Deepseekmath: Pushing the limits of mathematical reasoning in open language models, 2024.

[46] Haozhan Shen, Peng Liu, Jingcheng Li, Chunxin Fang, Yibo Ma, Jiajia Liao, Qiaoli Shen, Zilun Zhang, Kangjia Zhao, Qianqian Zhang, Ruochen Xu, and Tiancheng Zhao. Vlm-r1: A stable and generalizable r1-style large vision-language model, 2025.

[47] Amanpreet Singh, Vivek Natarajan, Meet Shah, Yu Jiang, Xinlei Chen, Dhruv Batra, Devi Parikh, and Marcus Rohrbach. Towards vqa models that can read. In *Proceedings of the IEEE/CVF conference on computer vision and pattern recognition*, pages 8317–8326, 2019.

[48] Charlie Victor Snell, Jaehoon Lee, Kelvin Xu, and Aviral Kumar. Scaling llm test-time compute optimally can be more effective than scaling model parameters. *ArXiv*, abs/2408.03314, 2024.

[49] Jiankai Sun, Chuanyang Zheng, Enze Xie, Zhengying Liu, Ruihang Chu, Jianing Qiu, Jiaqi Xu, Mingyu Ding, Hongyang Li, Mengzhe Geng, et al. A survey of reasoning with foundation models. *arXiv preprint arXiv:2312.11562*, 2023.

[50] Linzhuang Sun, Hao Liang, Jingxuan Wei, Bihui Yu, Tianpeng Li, Fan Yang, Zenan Zhou, and Wentao Zhang. Mm-verify: Enhancing multimodal reasoning with chain-of-thought verification, 2025.

[51] Kimi Team, Angang Du, Bofei Gao, Bowei Xing, Changjiu Jiang, Cheng Chen, Cheng Li, Chenjun Xiao, Chenzhuang Du, Chonghua Liao, et al. Kimi k1. 5: Scaling reinforcement learning with llms. *arXiv preprint arXiv:2501.12599*, 2025.

[52] Omkar Thawakar, Dinura Dissanayake, Ketan More, Ritesh Thawkar, Ahmed Heakl, Noor Ahsan, Yuhao Li, Mohammed Zumri, Jean Lahoud, Rao Muhammad Anwer, Hisham Cholakkal, Ivan Laptev, Mubarak Shah, Fahad Shahbaz Khan, and Salman Khan. Llamav-o1: Rethinking step-by-step visual reasoning in llms, 2025.

[53] Ke Wang, Junting Pan, Weikang Shi, Zimu Lu, Mingjie Zhan, and Hongsheng Li. Measuring multimodal mathematical reasoning with math-vision dataset, 2024.

[54] Xuezhi Wang, Jason Wei, Dale Schuurmans, Quoc Le, Ed Chi, Sharan Narang, Aakanksha Chowdhery, and Denny Zhou. Self-consistency improves chain of thought reasoning in language models. *arXiv preprint arXiv:2203.11171*, 2022.

[55] Jason Wei, Xuezhi Wang, Dale Schuurmans, Maarten Bosma, Brian Ichter, Fei Xia, Ed Chi, Quoc Le, and Denny Zhou. Chain-of-thought prompting elicits reasoning in large language models, 2023.

[56] Jinyang Wu, Mingkuan Feng, Shuai Zhang, Ruihan Jin, Feihu Che, Zengqi Wen, and Jianhua Tao. Boosting multimodal reasoning with mcts-automated structured thinking. *arXiv preprint arXiv:2502.02339*, 2025.

[57] Guowei Xu, Peng Jin, Hao Li, Yibing Song, Lichao Sun, and Li Yuan. Llava-cot: Let vision language models reason step-by-step, 2025.

[58] Yi Yang, Xiaoxuan He, Hongkun Pan, Xiyan Jiang, Yan Deng, Xingtao Yang, Haoyu Lu, Dacheng Yin, Fengyun Rao, Minfeng Zhu, Bo Zhang, and Wei Chen. R1-onevision: Advancing generalized multimodal reasoning through cross-modal formalization, 2025.

[59] Huanjin Yao, Jiaxing Huang, Wenhao Wu, Jingyi Zhang, Yibo Wang, Shunyu Liu, Yingjie Wang, Yuxin Song, Haocheng Feng, Li Shen, and Dacheng Tao. Mulberry: Empowering mllm with o1-like reasoning and reflection via collective monte carlo tree search, 2024.

[60] Shunyu Yao, Dian Yu, Jeffrey Zhao, Izhak Shafran, Thomas L. Griffiths, Yuan Cao, and Karthik Narasimhan. Tree of thoughts: Deliberate problem solving with large language models. *ArXiv*, abs/2305.10601, 2023.

[61] Qinghao Ye, Haiyang Xu, Guohai Xu, Jiabo Ye, Ming Yan, Yiyang Zhou, Junyang Wang, Anwen Hu, Pengcheng Shi, Yaya Shi, et al. mplug-owl: Modularization empowers large language models with multimodality. *arXiv preprint arXiv:2304.14178*, 2023.

[62] Xiang Yue, Yuansheng Ni, Kai Zhang, Tianyu Zheng, Ruoqi Liu, Ge Zhang, Samuel Stevens, Dongfu Jiang, Weiming Ren, Yuxuan Sun, Cong Wei, Botao Yu, Ruibin Yuan, Renliang Sun, Ming Yin, Boyuan Zheng, Zhenzhu Yang, Yibo Liu, Wenhao Huang, Huan Sun, Yu Su, and Wenhu Chen. Mmmu: A massive multi-discipline multimodal understanding and reasoning benchmark for expert agi, 2024.

[63] Eric Zelikman, Yuhuai Wu, Jesse Mu, and Noah Goodman. Star: Bootstrapping reasoning with reasoning. *Advances in Neural Information Processing Systems*, 35:15476–15488, 2022.

[64] Zhuosheng Zhang, Aston Zhang, Mu Li, Hai Zhao, George Karypis, and Alex Smola. Multimodal chain-of-thought reasoning in language models. *arXiv preprint arXiv:2302.00923*, 2023.

[65] Fan Zhou, Haoyu Dong, Qian Liu, Zhoujun Cheng, Shi Han, and Dongmei Zhang. Reflection of thought: Inversely eliciting numerical reasoning in language models via solving linear systems. *arXiv preprint arXiv:2210.05075*, 2022.

A Experiment Settings

A.1 Pipline Settings

A.1.1 Model Hyperparameter Settings

Our base model is Qwen2.5VL 7B[8], which supports dynamic resolution for input images. In all experiments, we constrained the pixel dimensions of each image to a minimum of 3136 pixels and a maximum of 1605632 pixels. Because the value of the bounding box is related to the number of pixels in the input image, the setting of the range of pixels needs to be unified.

A.1.2 Zoom Scaling Rule

In our pipeline, when a region is selected for closer inspection (e.g., via a "Crop" operation), a zoom operation is applied. The scaling factor for this zoom, denoted as scale, is determined dynamically based on the relative area of the selected bounding box (A_{bbox}) compared to the area of the original image (A_{orig}). Let $r = \frac{A_{\text{bbox}}}{A_{\text{orig}}}$ be this area ratio. The scale is calculated using the following piecewise function:

$$\text{scale} = \begin{cases} 2.0, & \text{if } r < 0.125 \\ 1.0, & \text{if } r \geq 0.5 \\ 2.0 - \dfrac{r - 0.125}{0.375}, & \text{otherwise} \end{cases} \tag{4}$$

This rule implies that smaller selected regions (smaller r) are scaled up more significantly (up to a factor of 2.0), while larger regions (larger r) are scaled up less, or not at all if they already occupy a substantial portion of the original image. The intermediate case provides a linear interpolation of the scaling factor.

A.2 Training Setting for Supervised Fine-tuning Stage

In the supervised fine-tuning stage, we used the complete VLIR dataset. Our experiments were conducted on 4 NVIDIA A100 GPUs, each equipped with 80GB of memory, leveraging DeepSpeed[41] for efficient training. We used a batch size of 2 with a gradient accumulation of 8, a learning rate of 2×10^{-7}, and trained for 3 epochs. During this phase, the vision encoder and MLP projector were frozen, and only the Large Language Model (LLM) component was trained.

A.3 Training Setting for R-GRPO Stage

For the R-GRPO stage, we sampled approximately 5,000 data points from TextVQA [47], GQA [17], VSR [25], DocVQA [32] and M^{3}CoT [9] datasets. Regarding the hyperparameters for the GRPO formulation(2), we set $M = 5$. Following the experience of related studies, we set $\beta = 0.0$, i.e., we eliminate the KL divergence constraint.

Our experiments for R-GRPO were performed on 6 NVIDIA A100 GPUs, each with 80GB of memory, also utilizing DeepSpeed[41]. The batch size per device was set to 1, with a gradient accumulation of 16. The learning rate was 1×10^{-6}, and training continued for 300 steps. We employ a rule-based reinforcement learning approach, where the correctness of the final answer was judged using an exact match criterion. Similar to the supervised fine-tuning stage, the vision encoder and MLP projector were frozen, and only the LLM component was trained.

B Prompt Templates for VLIR Dataset Construction and Filtering

B.1 Data Construction Prompts

Given an {image, question, answer} triplet, the following prompt was used to construct the interleaved visual-linguistic chain of thought:

```
You are performing "Multimodal Interleaved Reasoning". During the thinking
```

```
process, you need to keep an eye on the visual cues in the original image,
find regions of the image that help answer the question, and use the "Crop"
tool to crop and zoom in for detailed analysis.
When using the tool, you must output a JSON object in the following format:
{"bbox_2d": [x1, y1, x2, y2]}
Ensure that you "Crop" at least once.
Continue thinking after each operation until you reach the final answer.
Output the thinking process within a pair of <think> </think> tags and then
output the final answer within a pair of <answer> </answer> tags.
{question}
```

Listing 1: Prompt for dataset construction.

Given an {image, question, answer, bounding box annotation} quadruplet, the following prompt was used:

```
I will now provide you with an image, a question, and a "Crop" operation
string. Your task is to write the reasoning process used to answer the
question as instructed. During the reasoning process, the respondent
utilizes a "Crop" operation to assist with reasoning. The format of
the operation is as follows:
{"bbox_2d": [x1, y1, x2, y2]}
This bounding box indicates the key region that needs to be focused
on to correctly answer the question.
You must think step by step from the perspective of the respondent,
using the "Crop" operation at appropriate moments in your reasoning
process to eventually reach the correct answer. Important notes:
1. You must not modify the content or format of the "Crop" operation
in any way.
2. In a real setting, the respondent only has access to the image and
the question. This bounding box indicates the area where the correct
answer information is located. In this task, they are provided to ensure
the correctness of your reasoning process. When writing the reasoning,
pretend you are the respondent who independently identifies when to use
the "Crop" operation and how to reach the answer step by step.
3. Make sure the reasoning is fluent, logical, and concise.
4. Format of the reasoning process: <think>...</think><answer>...</answer>

Here is an example:
Question: Are there any black numbers or letters?
"Crop" operation: {"bbox_2d": [247, 384, 307, 444]}
Reasoning: <think>
Step 1: To determine if there are black numbers or letters, I need to
focus on the text visible in the image. The dog is wearing a heart-shaped
tag that has some text on it. I will crop and zoom in on the tag for a
closer look at the text details. {"bbox_2d": [247, 384, 307, 444]}
Step 2: After cropping, I can see that the letters "G PLUS" are in red,
and the numbers "6 223 13" are also in red. There are no black numbers
or letters on the tag. Review the rest of the image, there are no black
numbers or letters either.</think>
<answer>no</answer>

Question:{question}
"Crop" operation:{crop}
Now Output the reasoning process:
```

Listing 2: Prompt for dataset construction.

B.2 Data Filtering Prompts

The prompt for assessing the recognizability of the cropped images is as follows:

```
You need to determine whether the content in a picture is a complete and
semantically meaningful visual unit. Please look carefully at this cropped
image and determine whether it contains a recognizable object, block of text,
or specific part of a diagram. If it is recognizable, answer ’yes’; if not,
answer ’no’.
Now output ’yes’ or ’no’ directly.
```

Listing 3: Prompt for assessing cropped image recognizability.

The prompt for assessing the quality of the reasoning process is as follows:

```
You need to make an in-depth assessment of this reasoning process. First,
determine whether its logic is rigorous and whether each step of reasoning leads
naturally and smoothly to the next; second, check whether the reasoning process
progresses gradually towards arriving at the final answer; and lastly, check
whether there is any false information or repetitive redundancy in the text
that is not relevant to the reasoning. If this textual reasoning meets the
requirements in terms of logic, advancement and content streamlining, output
’yes’; whenever one of these is not met, output ’no’.
{question}
{ground-truth answer}
{reasoning process}
Now output ’yes’ or ’no’ directly.
```

Listing 4: Prompt for assessing reasoning process quality.

C Demonstrations for VLM-R³

This section provides qualitative examples illustrating the capabilities of VLM-R^3.

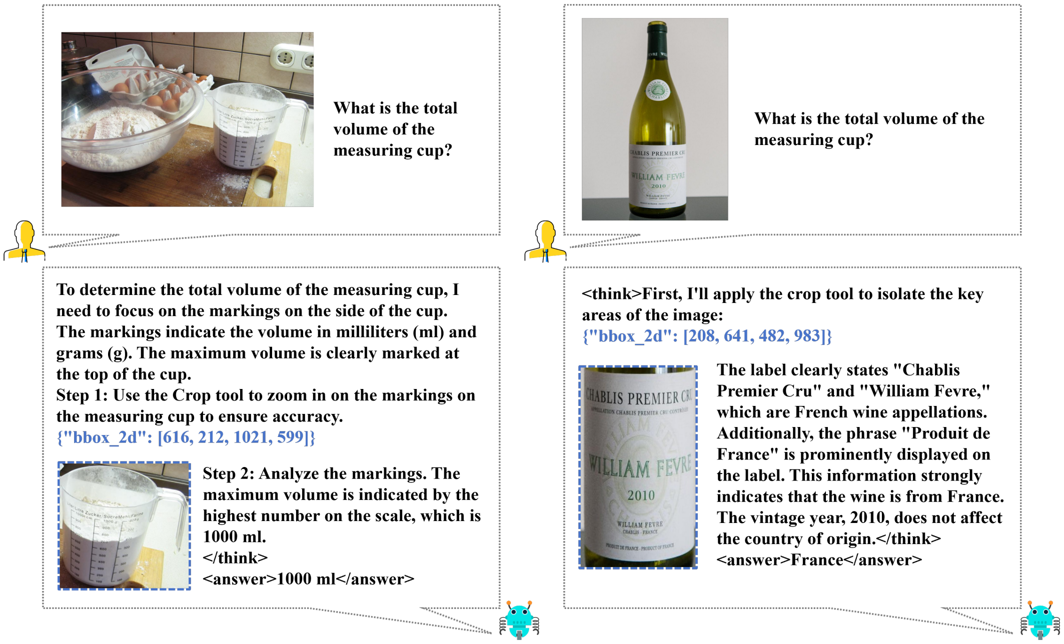

What is the total volume of the measuring cup?

To determine the total volume of the measuring cup, I need to focus on the markings on the side of the cup. The markings indicate the volume in milliliters (ml) and grams (g). The maximum volume is clearly marked at the top of the cup.
Step 1: Use the Crop tool to zoom in on the markings on the measuring cup to ensure accuracy.
{"bbox_2d": [616, 212, 1021, 599]}

Step 2: Analyze the markings. The maximum volume is indicated by the highest number on the scale, which is 1000 ml.
</think>
<answer>1000 ml</answer>

What is the total volume of the measuring cup?

<think>First, I'll apply the crop tool to isolate the key areas of the image:
{"bbox_2d": [208, 641, 482, 983]}

The label clearly states "Chablis Premier Cru" and "William Fevre," which are French wine appellations. Additionally, the phrase "Produit de France" is prominently displayed on the label. This information strongly indicates that the wine is from France. The vintage year, 2010, does not affect the country of origin.</think>
<answer>France</answer>

Figure 5: This figure presents how VLM-R^3 captures details in a natural image and reasons about them.

Add more figures as needed.

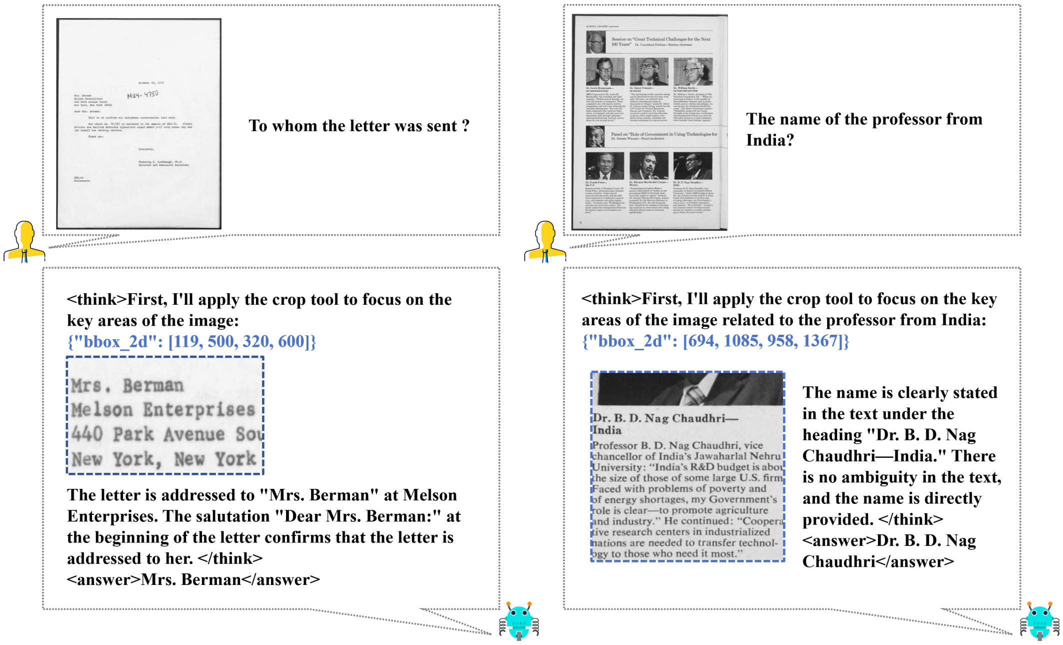

To whom the letter was sent ?

<think>First, I'll apply the crop tool to focus on the key areas of the image:
{"bbox_2d": [119, 500, 320, 600]}

Mrs. Berman
Melson Enterprises
440 Park Avenue Sou
New York, New York

The letter is addressed to "Mrs. Berman" at Melson Enterprises. The salutation "Dear Mrs. Berman:" at the beginning of the letter confirms that the letter is addressed to her. </think>
<answer>Mrs. Berman</answer>

The name of the professor from India?

<think>First, I'll apply the crop tool to focus on the key areas of the image related to the professor from India:
{"bbox_2d": [694, 1085, 958, 1367]}

Dr. B. D. Nag Chaudhri—
India
Professor B. D. Nag Chaudhri, vice
chancellor of India's Jawaharlal Nehru
University: "India's R&D budget is abou
the size of those of some large U.S. firm
Faced with problems of poverty and
of energy shortages, my Government's
role is clear—to promote agriculture
and industry." He continued: "Coopera
tive research centers in industrialized
nations are needed to transfer technol-
ogy to those who need it most."

The name is clearly stated in the text under the heading "Dr. B. D. Nag Chaudhri—India." There is no ambiguity in the text, and the name is directly provided. </think>
<answer>Dr. B. D. Nag Chaudhri</answer>

Figure 6: This figure presents how VLM-R^3 gets the text details from the document image.

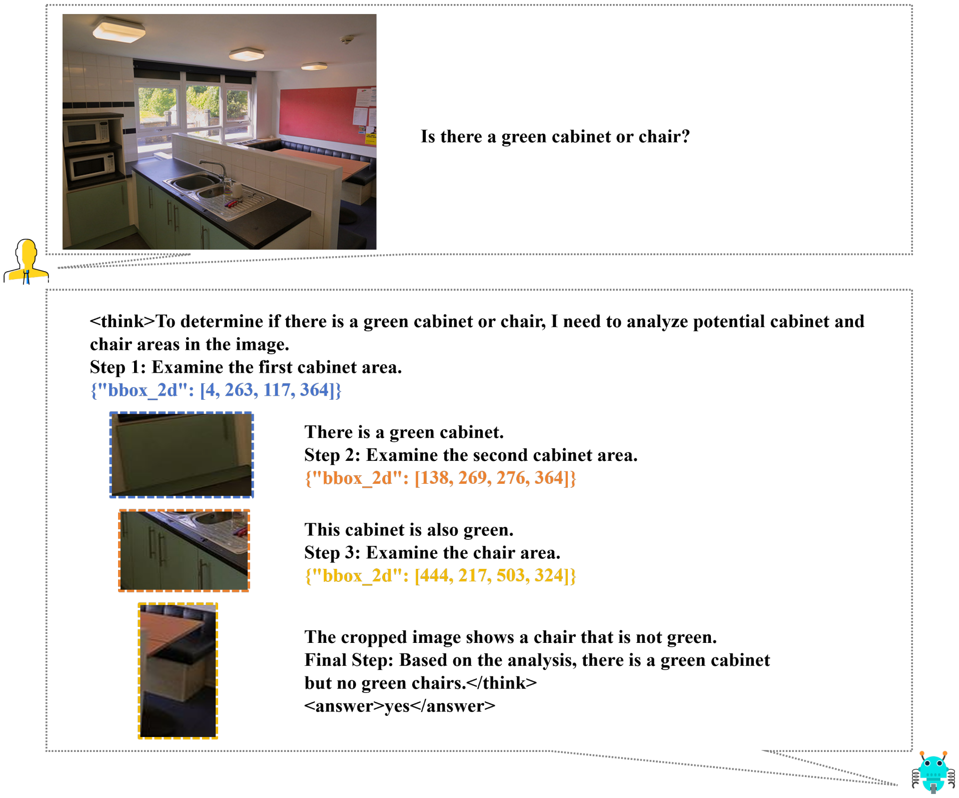

Is there a green cabinet or chair?

<think>To determine if there is a green cabinet or chair, I need to analyze potential cabinet and chair areas in the image.
Step 1: Examine the first cabinet area.
{"bbox_2d": [4, 263, 117, 364]}

There is a green cabinet.
Step 2: Examine the second cabinet area.
{"bbox_2d": [138, 269, 276, 364]}

This cabinet is also green.
Step 3: Examine the chair area.
{"bbox_2d": [444, 217, 503, 324]}

The cropped image shows a chair that is not green.
Final Step: Based on the analysis, there is a green cabinet but no green chairs.</think>
<answer>yes</answer>

Figure 7: This figure presents how VLM-R^3 iteratively tracks multiple visual cues in an image.

D Technical Appendices and Supplementary Material

Technical appendices with additional results, figures, graphs and proofs may be submitted with the paper submission before the full submission deadline (see above), or as a separate PDF in the

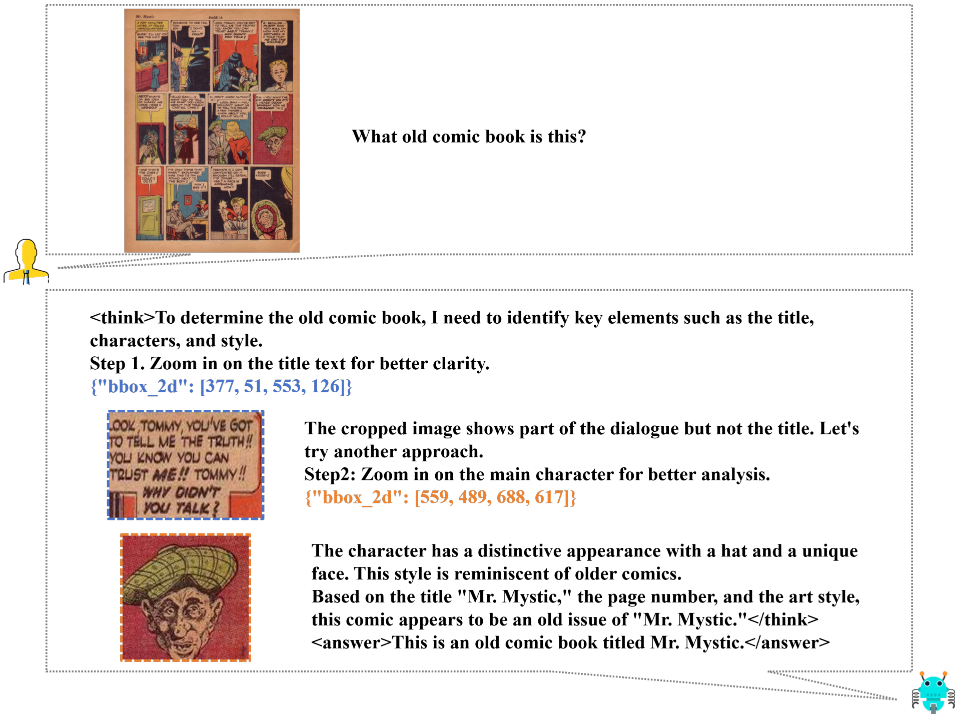

What old comic book is this?

<think>To determine the old comic book, I need to identify key elements such as the title, characters, and style.
Step 1. Zoom in on the title text for better clarity.
{"bbox_2d": [377, 51, 553, 126]}

LOOK TOMMY, YOU'VE GOT TO TELL ME THE TRUTH!! YOU KNOW YOU CAN TRUST ME!! TOMMY!! WHY DIDN'T YOU TALK?

The cropped image shows part of the dialogue but not the title. Let's try another approach.
Step2: Zoom in on the main character for better analysis.
{"bbox_2d": [559, 489, 688, 617]}

The character has a distinctive appearance with a hat and a unique face. This style is reminiscent of older comics.
Based on the title "Mr. Mystic," the page number, and the art style, this comic appears to be an old issue of "Mr. Mystic."</think>
<answer>This is an old comic book titled Mr. Mystic.</answer>

Figure 8: This figure presents how VLM-R^3 performs complex interleaved text-image CoT reasoning.

ZIP file below before the supplementary material deadline. There is no page limit for the technical appendices.

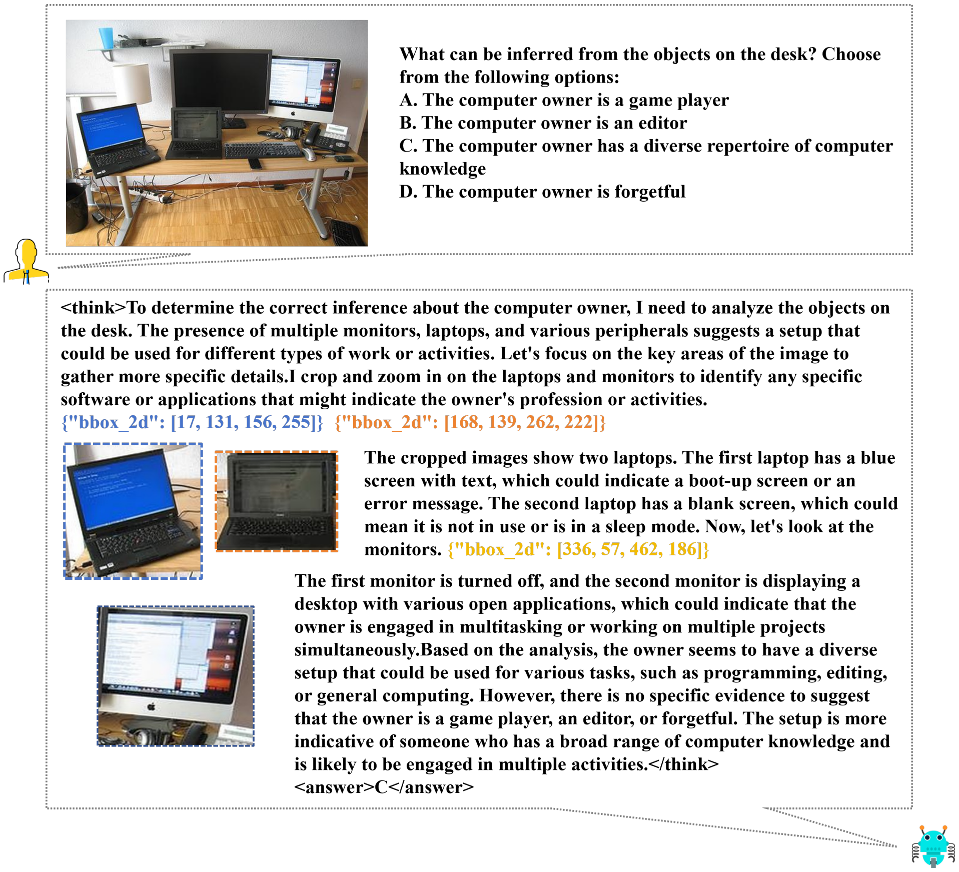

What can be inferred from the objects on the desk? Choose from the following options:
A. The computer owner is a game player
B. The computer owner is an editor
C. The computer owner has a diverse repertoire of computer knowledge
D. The computer owner is forgetful

<think>To determine the correct inference about the computer owner, I need to analyze the objects on the desk. The presence of multiple monitors, laptops, and various peripherals suggests a setup that could be used for different types of work or activities. Let's focus on the key areas of the image to gather more specific details.I crop and zoom in on the laptops and monitors to identify any specific software or applications that might indicate the owner's profession or activities.
{"bbox_2d": [17, 131, 156, 255]} {"bbox_2d": [168, 139, 262, 222]}

The cropped images show two laptops. The first laptop has a blue screen with text, which could indicate a boot-up screen or an error message. The second laptop has a blank screen, which could mean it is not in use or is in a sleep mode. Now, let's look at the monitors. {"bbox_2d": [336, 57, 462, 186]}

The first monitor is turned off, and the second monitor is displaying a desktop with various open applications, which could indicate that the owner is engaged in multitasking or working on multiple projects simultaneously.Based on the analysis, the owner seems to have a diverse setup that could be used for various tasks, such as programming, editing, or general computing. However, there is no specific evidence to suggest that the owner is a game player, an editor, or forgetful. The setup is more indicative of someone who has a broad range of computer knowledge and is likely to be engaged in multiple activities.</think>
<answer>C</answer>

Figure 9: This figure presents how VLM-R^3 performs complex interleaved text-image CoT reasoning.